Dr. K. W. Wong*
E. V. Gamble
R. E. Riggins
University of Illinois
Urbana, Illinois 61801

Analysis of RBV Television System

Preliminary results for simulated ERTS photographs showed that the total geometric distortion was ±0.445 mm and the random components were only 0.018 mm.

Introduction

The return-beam vidicon (RBV) television camera is a high-resolution TV camera developed by the Astro-Electronics Division of the Radio Corporation of America (RCA). Three such cameras are flying on board the first earth resources technology satellite (ERTS-I) which was launched by NASA in 1972. The three TV cameras are boresighted to provide images of the same scene in three separate spectral bands. The television signal is transmitted back to a ground receiving station where film copies of the TV pictures are reconstructed using an electron beam recorder (EBR). Each TV frame consists of 4200 TV lines. A reseau pattern of 81 points arranged in a rectangular array of 9 rows and 9 columns appears in every frame of RBV images. The orbital data for ERTS-I is summarized in Table 1, and the characteristics of the RBV-EBR system is given in Table 2. More detailed descriptions of the ERTS-I mission can be found in References 1, 2 and 3.

It has been recognized by NASA and the U.S. Geological Survey that the RBV photographs from ERTS-I can be used to produce small-scale planimetric maps which will be of vital interest to all users of ERTS-I data including geologists, hydrologists, planners, etc. For this reason, the Bendix Research Laboratories has been contracted by NASA to develop automatic image processing equipment which will be used to correct the geometric distortions and to print the processed images into cartographic format. The principles of the Bendix image processing system have been reported by Dr. Robert Forrest[4].

The full impact of the RBV-EBR system on surveying and mapping reaches far beyond the ERTS-I mission. Although a second mission, called ERTS-B, is scheduled to follow ERTS-I a year later, both of these missions are primarily experimental satellites. It is highly probable that in the future a series of such satellites will be operated on a continuous basis to provide regular observations of the earth's environment. With the increasing importance of environmental control and re-

Abstract: *Three RBV television cameras are being flown on board the first Earth Resources Technology Satellite (ERTS-I). Preliminary studies using laboratory RBV images showed that the total geometric distortion amounted to about ±0.445 mm (8.2 TV-lines) at one-sigma level, and the random component was about ±0.018 mm (0.3 TV-line). The systematic distortion over the entire frame of RBV picture was successfully modeled using a pair of 20-term polynomials with a residual error of ±0.030 mm (0.6 TV-line). Simulation studies on pre-flight calibration showed that the focal length could be determined to within ±0.020 mm under the various system constraints in ERTS. But due to the narrow field angle of the TV camera, the position of the principal point could be determined to within ±5 μm only if the direction of the optical axis was constrained to within ±10 seconds of arc.*

* Presented at the Annual Convention of the American Society of Photogrammetry, Washington, D.C., March 1972.

TABLE 1. ORBITAL DATA FOR ERTS-I

Parameter	*Data*
Altitude	912 km. ±0.927 km. in orbit ±0.062 km. in spheroid deviation
Attitude	±0.7° on any axis correctable to ±0.1°
Positioning by empheries	±0.257 km.
Positioning by photogrammetric resection	about 0.1 km.
Orbit inclination	99.092° with a 3 sigma error of ±0.25°
Expected life	1 year
Period	6196.015 seconds
Time at ascending node	21:30 local

TABLE 2. CHARACTERISTICS OF THE RBV TELEVISION SYSTEM

Parameter	*System Accuracy*
Max. optical lens distortion	±30 μm
Reseau coordinates	±2 μm (calibration)
Equivalent focal length	125.98 mm. $\pm \frac{0.270}{0.980}$ mm.
Geometric stability of NASA/EBR	0.1%
Resolution	60-70 line-pairs/mm.
Picture smear	½ TV line
Max. image distortion	1%
Max. deflection skew	±0.5%
Max. size and centering shift	±1%
No. of scan lines	4200
Field of view (diagonal)	16.22°

sources inventory, and with the advent of automatic image processing techniques such as density slicing, topographic and thematic mapping from space photographs is increasingly becoming a real necessity.

Furthermore, the RBV-EBR system also holds excellent promise as a mapping system in the mapping of other planets such as the moon, Mars, and Venus. It also represents an advanced TV photographic system which is approaching the resolution and geometric fidelity required for mapping applications in many areas of scientific and industrial research. The ERTS-I mission thus provides an excellent opportunity to exploit fully the mapping capability of a high-resolution, high-quality TV system.

The general objectives and problems of performing geometric calibration of the RBV system for ERTS-I have been discussed by Dr. Robert McEwen of the USGS[5]. This paper describes the work performed during Phase I of a research program which is being conducted at the University of Illinois at Urbana-Champaign under the sponsorship of USGS. Eighteen frames of experimental RBV images were analyzed to determine the general magnitude and pattern of geometric distortions. Although a laser beam image recorder (LBIR) was used as hardcopy output device in producing these preliminary copies instead of the EBR, the photographs should provide a preliminary indication on the general distortion characteristics of the RBV camera. Several analytical methods for modeling the geometric distortions were also tested. In addition, simulation studies were conducted to estimate the potential accuracy of pre-flight and in-flight calibration of the internal geometry of the RBV system.

GEOMETRIC DISTORTION CHARACTERISTICS

Previous theoretical and experimental studies had shown that geometric distortions in TV images could be highly systematic and remain stable from frame to frame.[6,7] An analytical method had also been developed by Dr. Wong for determining the random and systematic components of distortions from a group of successive exposures. This method[7] was used to analyze the distortion characteristics of an experimental RBV camera system.

Eighteen frames of RBV images in 9 × 9-

inch transparencies were obtained from USGS through the courtesy of RCA Laboratories. These frames were made from a laboratory model of RBV camera, and a laser beam image recorder (LBIR) was used as hard-copy output device instead of an electron beam recorder. All 18 frames were made from the same RBV tube.

Frames 1 to 10 all had a clear field with no photographic content besides the 81 reseau points, whereas frames 11 to 18 contained a resolution pattern. The coordinates of the 81 reseau points on the photoconductive target of the camera tube were calibrated at the USGS with an accuracy of ± 2 μm.

The image coordinates of the reseau points on the 18 frames were measured on a Wild STK-1 stereocomparator operating in a monoscopic mode. The comparator had a least count of 1 μm and the standard deviation of the image measurements was found to be ± 5 μm on the 9 $\times$ 9-inch format for frames 1 to 10 and ± 7 μm for frames 11 to 18. The lower measurement accuracy for the second set of frames was largely due to image degradation caused by the resolution pattern. The edges of the reseau generally appeared less sharp than those in frames 1 to 10. The following average results were obtained from the 18 frames:

1) Total geometric distortions:
$\sigma_x = \pm 0.445$ mm. $= \pm 8.2$ TV-Lines
$\sigma_y = \pm 0.503$ mm. $= \pm 9.3$ TV-Lines.

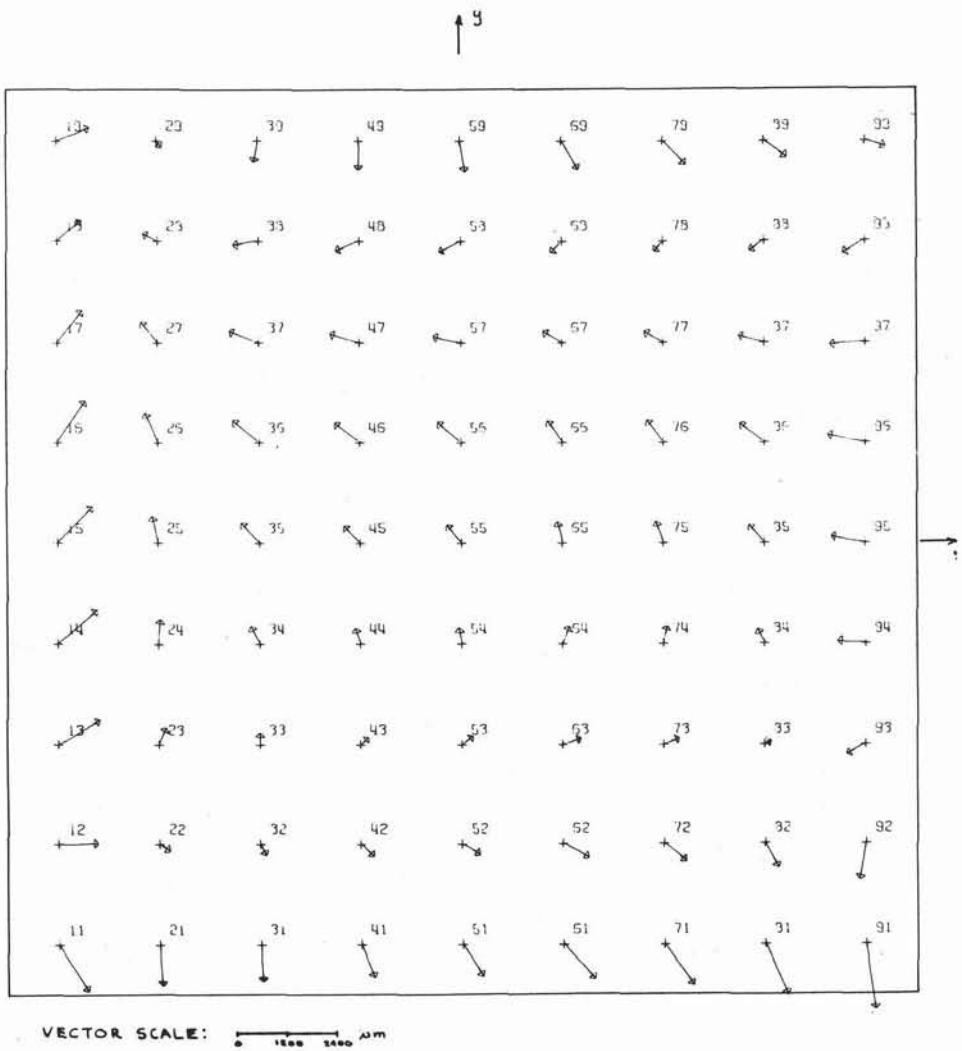

FIG. 1. Systematic component of distortions from Frames 11 to 18.

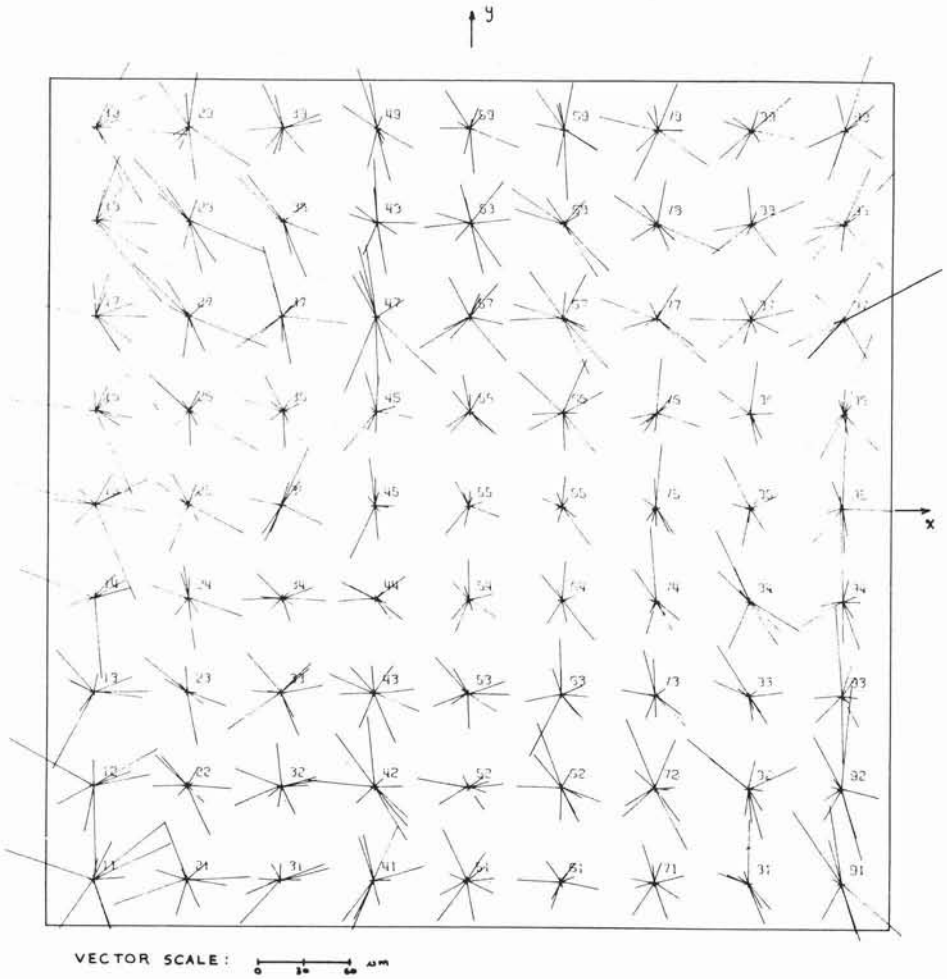

FIG. 2. Random components of distortions from Frames 11 to 18.

2) Total geometric distortions after differential scale corrections:
σ_X (after scale correction) = ± 0.442 mm. = $\pm$ 8.2 TV-Lines
σ_Y (after scale correction) = ± 0.480 mm. = $\pm$ 8.9 TV-Lines.
By comparing the results in (1) and (2), it was concluded that there was negligible scale difference in the horizontal and vertical directions of the RBV images.
3) Random components of distortions:
σ_X random = $\pm$ 0.016 mm. = $\pm$ 0.3 TV-Lines
σ_Y random = $\pm$ 0.018 mm. = $\pm$ 0.3 TV-Lines.

As the 9 × 9-inch frame was a 9.1 times enlargement of the vidicon target plate, the random distortions on the target scale thus amounted to:

σ_X random at target scale = ± 0.002 *mm.*
σ_Y random at target scale = ± 0.002 *mm.*

Because the positions of the reseau points themselves were calibrated to only ± 2 μm, the geometric distortion may therefore be considered as completely stable between frames. Figure 1 is a map of the systematic distortions in frames 11 to 18. Figure 2 shows the corresponding random distortions at each reseau point for the 8 frames.

The above results must be considered preliminary as only a limited number of frames were used for the analysis, and the RBV camera was still under development and engineering testing. It is also to be remembered that these frames were reproduced on a laser beam image recorder. The ERTS-1 system is using an electron beam recorder as output device. Nevertheless, the analysis did show that excellent geometric stability can be achieved.

Image Correction Method

The highly systematic nature of the geometric distortions suggested that image correction procedures could be developed to restore the geometric fidelity of the TV images. Several image correction procedures were investigated with the hope that the results would provide some guidelines for the future development of analog and analytical image processing techniques.

SUB-FRAME APPROACH

An RBV frame may be subdivided into sub-frames with each sub-frame containing four reseau marks. Then by comparing the measured image coordinates of the reseau marks with their corresponding calibrated coordinates, the distortion within this sub-frame may be modeled by a set of polynomials as follows:

$$\bar{x}_j = a_0 + a_1 x_j + a_2 y_j + a_3 x_j y_j \quad (1)$$

$$\bar{y}_j = b_0 + b_1 x_j + b_2 y_j + b_3 x_j y_j \quad (2)$$

where x_j *and* y_j are image coordinates of a reseau point j; and $\bar{x}_j$ and $\bar{y}_j$ are the corresponding calibrated coordinates. Four sets of reseau coordinates yield eight equations and a unique solution can be obtained for the unknown coefficients in the above distortion model. The computed coefficients may then be used to correct every point within the sub-frame. One big disadvantage of this approach is that all 81 reseau points must be measured in every frame.

No attempt was made to test the accuracy of this method because it would require RBV photography of a calibrated grid or a control field.

DISTORTION CORRECTION TABLE

This method is a modification of the sub-frame approach and is designed for processing a limited number of image points within each photographic frame.

A set of 10 frames may be chosen from one day's RBV photographs. The image coordinates of the reseau points on these 10 frames are measured to determine the systematic distortions at the 81 reseau points. These distortion figures can then be used as a distortion table in the image correction process.

Let x_j and y_j be the raw measured image coordinates of a point j. A search is made through the distortion table to locate the four nearest reseau points and the systematic distortions at those locations. The coefficients in the following set of polynomials may then be computed using a least-square procedure:

$$\dot{r}_{x_i} = a_0 + a_1 \bar{x}_i + a_2 \bar{y}_i \quad (3)$$

$$\dot{r}_{y_i} = b_0 + b_1 \bar{x}_i + b_2 \bar{y}_i \quad (4)$$

where $\bar{x}_i$ and $\bar{y}_i$ are the calibrated coordinates of a reseau point i, and $\dot{r}_{xi}$ and $\dot{r}_{yi}$ are the systematic distortion at point i. Having determined the coefficients a_0, a_1, a_2, b_0, b_1, and b_2, the expected systematic distortion at point j is then computed as

$$\dot{r}_{x_j} = a_0 + a_1 x_j + a_2 y_j \quad (5)$$

$$\dot{r}_{y_j} = b_0 + b_1 x_j + b_2 y_j \quad (6)$$

and the image coordinates are corrected as follows:

$$\bar{x}_j = x_j - \dot{r}_{x_j} \quad (7)$$

$$\bar{y}_j = y_j - \dot{r}_{y_j}. \quad (8)$$

One big advantage of this method is that it does not require that all 81 reseau points be measured in the photographic frame being processed. If the systematic component of distortion is stable as indicated by the previous results, the same distortion table can be used for a week or month. However, this method is practicable only if there are few points to be processed as in the case of analytical triangulation. As the number of image points to be processed increases, the amount of computation become prohibitively large.

This method was coded into a computer program and was tested using frames number 3, 4, 5, 6, 7 and 8. The systematic distortions computed from frames 1 to 10 were used as distortion correction table. The raw measured image coordinates for each reseau point in frames 3 to 8 were then corrected according to the above procedure. The mean standard errors of the corrected x and y coordinates were $\pm$ 34 μm and $\pm$ 39 μm respectively.

Inasmuch as the random distortions alone amounted to 16 μm, this method did seem to have excellent potential accuracy. However, its ultimate usefulness can only be tested with RBV photographs of a calibrated grid or control field. As a practical method of image correction, however, this approach is definitely inferior to the full-frame polynomial method to be described in the following section.

FULL-FRAME POLYNOMIALS

This method attempts to model the distortions over the entire frame using a pair of

polynomials. The following general polynomials were used:

$$\dot{r}_x = a_1 + a_2x + a_3y + a_4xy + a_5x^2 + a_6y^2 + a_7x^2y + a_8xy^2 + a_9x^3 + a_{10}y^3 + a_{11}x^3y + a_{12}xy^3 + a_{13}x^4 + a_{14}y^4 + a_{15}x^2y^2 + a_{16}x^3y^2 + a_{17}x^2y^3 + a_{18}x^5 + a_{19}y^5 + a_{20}x^3y^3 \quad (9)$$

$$\dot{r}_y = b_1 + b_2x + b_3y + b_4xy + \cdots + b_{20}x^3y^3. \quad (10)$$

Various cases were tested in which the number of terms used in the polynomials varied from 10 to 20. For cases one, two and three; the first 10, 12, and 15 terms were used, respectively. All 20 terms were used in both Cases 4 and 5, but in Case 5 the outermost rows and columns of the reseau were omitted from consideration. The case data and standard deviations of the residuals are listed in Table 3.

The results show that the full-frame polynomial approach had excellent accuracy for modelling systematic distortions in the RBV image. Third-degree polynomials including 10 terms in each of x and y polynomials were sufficient to achieve a modelling accuracy of ± 0.079 mm. Increasing the number of terms to 12 and 14 did not show any appreciable improvement. However, if 20 terms were used, the standard errors in x and y were reduced to ± 30 μm and $\pm 28\mu$m respectively. Even more surprising was the accuracy obtained if the outside rows and columns of reseau were omitted. The distortion was modelled to within ± 9 μm which was equivalent to ± 1 μm on the camera target. This method may have significant impact on the design of image processors and will be tested more rigorously using additional RBV imageries.

The polynomials in Equations 9 and 10 are only slight modifications of the distortion equations originally recommended by Dr. Wong.[6]

OTHER APPROACHES

Three other approaches were attempted. They involved dividing a frame into horizontal bands in a direction parallel to the scan lines. Separate polynomials were then used to model the distortions within each band. If such polynomials can adequately describe the distortion pattern, it may be possible to modulate the scanning signal in the same manner so that geometric distortion can be eliminated directly at the electron beam recorder.

The first approach divided the frame into nine bands with a row of reseau located at the center of each band. This method was referred to as the *single-line* method.

The second approach subdivided the frame into eight overlapping, horizontal bands with band one covering rows 1 and 2 of the reseau, band two covering rows 2 and 3, band three covering rows 3 and 4 and so on. This was referred to as the *double-line* method.

The third approach, called the *triple-line* method, subdivided the frames into horizontal bands containing rows 1, 2 and 3; 3, 4 and 5; 5, 6 and 7; and 7, 8 and 9.

Polynomials having various numbers of terms were tested for each of the three approaches. Table 4 gives a summary of the results. Only the single-line method had results within the tolerable range of accuracy.

PRE-FLIGHT CALIBRATION

The objective of pre-flight calibration is to determine the interior geometry of the RBV cameras after the components have been assembled together. The parameters to be determined include (1) the equivalent focal length, (2) the coordinates of the principal point, and (3) the lens distortion characteristics. Figure 3 illustrates the geometric relationship between the measured and the unknown parameters in the calibration problem. The reseau coordinates x_j, y_j are to be measured with an accuracy of ± 2 μm. The horizontal α_j and vertical β_j angles to the 81 reseau points are to be measured using the

TABLE 3. TEST CASES FOR FULL-FRAME POLYNOMIALS

Case	*Unknowns*	*Equations*	*Degrees of Freedom*	σ_x(mm)	σ_y(mm)
1	20	162	142	.079	.076
2	24	162	138	.079	.076
3	28	162	134	.079	.038
4	40	162	122	.030	.028
5	40	98	58	.009	.009

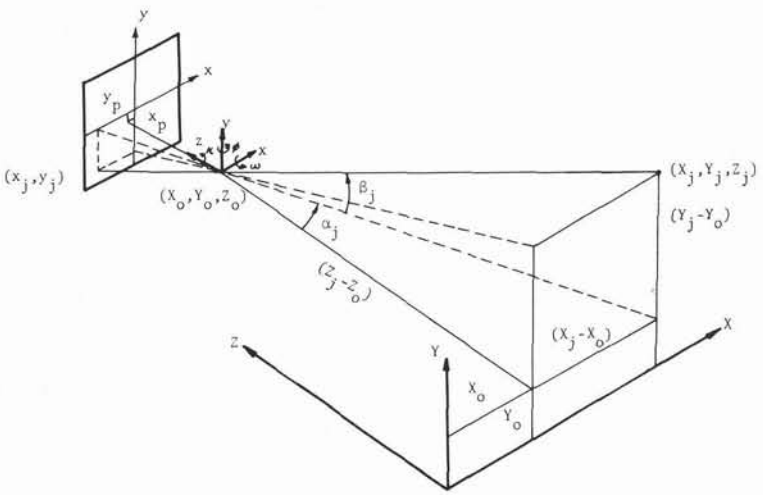

FIG. 3. Geometry of pre-flight calibration.

goniometer principle. The angular measurements are expected to have an accuracy of about 2 seconds of arc.

The familiar projective transformation equations may be used to express the relationship between the reseau points and their corresponding angular directions. The basic observation equations are as follows:

$$x_j + x_j[l_1 r^2 + l_2 r^4 + l_3 r^6] + [\rho_1(r^2 + 2x_j^2) + 2\rho_2 x_j y_j][1 + \rho_3 r^2] - x_p + f \times \left[\frac{m_{11}\sin\alpha_j\cos\beta_j + m_{12}\sin\beta_j + m_{13}\cos\alpha_j\cos\beta_j}{m_{31}\sin\alpha_j\cos\beta_j + m_{32}\sin\beta_j + m_{33}\cos\alpha_j\cos\beta_j}\right] = 0$$

and

$$y_j + y_j[l_1 r^2 + l_2 r^4 + l_3 r^6] + [2\rho_1 x_j y_j + \rho_2(r^2 + 2y_j^2)][1 + \rho_3 r^2] - y_p + f \times \left[\frac{m_{21}\sin\alpha_j\cos\beta_j + m_{22}\sin\beta_j + m_{23}\cos\alpha_j\cos\beta_j}{m_{31}\sin\alpha_j\cos\beta_j + m_{32}\sin\beta_j + m_{33}\cos\alpha_j\cos\beta_j}\right] = 0$$

where x_j and y_j are calibrated coordinates of the reseau point j, α_j and β_j are the corresponding horizontal and vertical angle of light ray from point j, l_1, l_2, l_3, ρ_1, ρ_2 and ρ_3 are the unknown coefficients of the lens distortion model, $r^2 = (x_j^2 + y_j^2)$, the m_{ij}'s are functions of the direction of the optical axis of the lens system, f is the unknown focal length, and x_P, y_P are the unknown coordinates of the principal point.

A computer program based on the method of weighted least-square adjustment was developed, and fictitious data were generated to test the calibration technique under several conditions of measurement accuracy and system constraints. Three test cases were conducted for the RBV camera configuration (16.22° field) and three test cases were conducted for a camera with the same focal length but a 45° field. The latter cases were included to study the effect of the narrow field angle of the RBV camera on the mathematical solution. The results are summarized in Tables 3 and 4. Lens distortions were included only in Cases 3, 6 and 7.

TABLE 4. TEST CASES FOR BAND POLYNOMIALS

Approach	Case	No. of Bands	Per Band Unknowns	Per Band Equations	Df.	Mean σ_x(mm)	σ_y(mm)
Single-Line	1	9	12	18	6	.070	.030
Double-Line	1	8	12	36	24	.134	.319
	2	8	16	36	20	.103	.245
	3	8	20	36	16	.997	.289
Triple-Line	1	4	12	54	42	.144	.308
	2	4	16	54	38	.093	.265
	3	4	20	54	34	2.420	2.302

The following observations were made from these simulation results:

- Under the conditions tested, the focal length could be calibrated with an accuracy well within the ± 20 μm requirement.
- Because of the narrow field angle, a major part of the lens distortion was compensated by a small error in the calibrated focal length.
- In order to meet the accuracy requirement of ± 5 μm for the coordinates x_p and y_p of the principal point, the direction of optical axis, defined by ω, φ and κ, must be measured to about ± 10 seconds of arc. This requirement was due primarily to the narrow field angle of the RBV camera which resulted in poor geometrical condition for the solution. In the case of a 45° camera, the coordinates x_p and y_p could be determined to within ± 0.5 μm while the direction of the optical axis was constrained to only ± 1800 sec.

In-Flight Calibration

The objective of in-flight calibration is to provide periodic checks on the internal geometry of the RBV cameras during the life of the satellite. The method used for the calibration of conventional aerial cameras can be adopted directly for this application. A test site with a dense network of ground controls can be set up. Then by measuring the image coordinates of these ground control points on selected frames of RBV images, the internal geometry can be computed by conventional means. The accuracy of such in-flight calibration will depend on the accuracy of the following parameters: (1) image coordinates of the ground control points, (2) ground coordinates of the control points, (3) position X^c, Y^c, Z^c of the satellite from tracking data, and (4) attitude ω, φ, κ of the satellite.

Table 5 lists the simulation results under various combinations of measurement accuracy and constraints. The image coordinates were assumed to have an accuracy of ± 0.020 mm. (at a 9 × 9-inch format) in Cases 1 to 4, and ± 0.20 mm. in Case 5. Preliminary results in geometric distortions, as discussed in the previous paragraphs, had already shown that an image accuracy of ± 0.020 mm. after refinement was within the capability of the system. Case 5 represented the situation in which the ground controls could not be identified accurately on the RBV photography.

At a 9 × 9-inch format, the accuracy requirements for camera calibration are: (1) $\sigma_{xp} = \sigma_{yp} = \pm 0.045$ mm. and (2) $\sigma_f = \pm 0.180$ mm. By comparing these figures with the results in Table 7, the following observations were made:

- ★ If the geometry of the RBV imagery could be restored to within ± 20 μm, in-flight calibration could determine the focal length within the desired accuracy.
- ★ Even if the image coordinates were corrected to ± 20 μm and the camera attitude known to $\pm 0.1°$, the position of the principal point could not be determined to the desired accuracy of ± 0.045 mm. An accuracy of ± 1.0 mm seemed to be a more reasonable goal for in-flight calibration.

Summary of Conclusions

Eighteen frames of RBV imageries were measured and analyzed, and the geometric distortion was found to be highly systematic and stable in nature. The total geometric distortion amounted to ± 0.445 mm at one-sigma level, and the random components amounted to only ± 0.018 mm. However, these results must be considered as preliminary. The images were obtained when the RBV system was still under development, and they were produced by a laser beam image recorder rather than by an electron beam recorder.

The systematic distortion over an entire frame of RBV picture was successfully modelled using a pair of 20-term polynomials with an accuracy of ± 0.030 mm in σ_x and ± 0.028 mm in σ_y. If the outermost rows and columns of reseau were omitted from consideration, the modelling accuracy increased to ± 0.009 mm in σ_x and σ_y. This method will be more rigorously tested when more RBV images become available.

A limited simulation study on pre-flight calibration showed that the focal length could be easily calibrated to the desired accuracy of ± 20 μm. However, due to the narrow field angle of the cameras, there was strong correlation between the parameters x_p, y_p defining the position of the principal point and the orientation angles ω, φ, κ of the optical axis. The position of the principal point could be determined to within ± 5 μm only if the direction of the optical axis was known to within ± 10 seconds of arc.

If the geometry of the RBV images was assumed to be restored to within ± 20 μm in 9 × 9-inch format, in-flight calibration could determine the focal length within the desired accuracy of ± 20 μm at target scale (or ± 0.180 mm. at a 9 × 9-inch format). However, within the constraint of $\pm 0.1°$ in camera attitude, it seemed that the principal

TABLE 5. CALIBRATION ACCURACY FOR RBV CAMERAS (16.22° FIELD)

Case	*Measurement Accuracy*	*Constraints*	*Computed Parameters & RMS Errors*					
			x_p (*mm.*)	y_p (*mm.*)	f (*mm.*)	ω (*sec.*)	ϕ (*sec.*)	κ (*sec.*)
1	$\sigma_{x_j} = \sigma_{y_j} = 1$ μm.	$\sigma_{x_p} = \sigma_{y_p} = \pm .100$ mm.	.014	.021	125.999	34″	−23″	.6″
	$\sigma_{\alpha_j} = \sigma_{\beta_j} = 1$ sec.	$\sigma_\omega = \sigma_\phi = \sigma_\kappa = \pm 1800$ sec.	±.018	±.019	±.001	±30″	±30″	±1.7″
2	$\sigma_{x_j} = \sigma_{y_j} = 2$ μm.	Same as Case 1	.024	.035	125.999	57″	−40″	1″
	$\sigma_{\alpha_j} = \sigma_{\beta_j} = 2$ sec.		±.033	±.033	±0.002	±54″	±54″	±3″
3	$\sigma_{x_j} = \sigma_{y_j} = 2$ μm.	$\sigma_{x_p} = \sigma_{y_p} = \pm 0.100$ mm.	−.003	.003	125.964	5″	4″	.5″
	$\sigma_{\alpha_j} = \sigma_{\beta_j} = 3$ sec.	$\sigma_\omega = \sigma_\phi = \sigma_\kappa = \pm 10$ sec.	±.004	±.004	±.018	±6″	±6″	±3″

TABLE 6. CALIBRATION ACCURACY FOR A CAMERA WITH 45° FIELD

Case	*Measurement Accuracy*	*Constraints*	*Computed Parameters and RMS Errors*					
			x_p (*mm.*)	y_p (*mm.*)	f (*mm.*)	ω (*sec.*)	ϕ (*sec.*)	κ (*sec.*)
4	$\sigma_{x_j} = \sigma_{y_j} = 1$ μm.	$\sigma_{x_p} = \sigma_{y_p} = \pm 0.100$ mm.	.0005	.0003	126.000	0.48	−.6	−.13
	$\sigma_{\alpha_j} = \sigma_{\beta_j} = 1$ sec.	$\sigma_\omega = \sigma_\phi = \sigma_\kappa = \pm 1800$ sec.	±.0003	±.003	±.0002	±.4	±.4	±.18
5	$\sigma_{x_j} = \sigma_{y_j} = 2$ μm.	Same as Case 3	−.0012	−.0006	126.000	−.8	1.5	.3
	$\sigma_{\alpha_j} = \sigma_{\beta_j} = 1$ sec.		±.0005	±.0005	±.0003	±.5	±.5	±.3
6	Same as Case 4	Same as Case 4	−.0012	−.0006	126.000	−.8	1.5	.3
			±.0005	±.0005	±.001	±.5	±.5	±.3
7	$\sigma_{x_j} = \sigma_{y_j} = 2$ μm.	Same as Case 3	−.0019	−.0002	125.999	−.2	2.4	.7
	$\sigma_{\alpha_j} = \sigma_{\beta_j} = 3$ sec.		±.001	±.001	±.005	±1.1	±1.2	±.6

TABLE 7. EXPECTED ACCURACY OF IN-FLIGHT CALIBRATION

Case	*Measurement Accuracy*	*Constraints*	*RMS Error in 9-inch Frame Format*					
			$\sigma_{x_p} = \sigma_{y_p}$ (*mm.*)	σ_f (*mm.*)	$\sigma_\omega = \sigma_\phi$ (*sec.*)	σ_κ (*sec.*)	$\sigma_{X^c} = \sigma_{Y^c}$ (*sec.*)	σ_{Z^c} (*sec.*)
1	$\sigma_x = \sigma_y = \pm .02$ mm. $\sigma_{\text{ground}} \pm 2$ m.	$\sigma_{x_p} = \sigma_{y_p} = \pm 10.0$ mm. $\sigma_f = \pm 10.0$ mm. $\sigma_{X^c} = \sigma_{Y^c} = \sigma_{Z^c} = \pm 1000$ m. $\sigma_\omega = \sigma_\phi = \sigma_\kappa = \pm 3600$ sec.	1.509	1.226	157	10	992	992
2	$\sigma_x = \sigma_y = \pm .02$ mm. $\sigma_g = \pm 2$ m.	$\sigma_{x_p} = \sigma_{y_p} = \pm 10.0$ mm. $\sigma_f = \pm 10.0$ mm. $\sigma_{X^c} = \sigma_{Y^c} = \pm 100.0$ m. $\sigma_{Z^c} = \pm 30.0$ m. $\sigma_\omega = \sigma_\phi = \sigma_\kappa = \pm 360.0$ sec.	.805	.097	144	10	100	30
3	$\sigma_x = \sigma_y = \pm .02$ mm. $\sigma_g = \pm 2$ m.	$\sigma_{x_p} = \sigma_{y_p} = \pm .045$ mm. $\sigma_f = \pm .180$ mm. $\sigma_{X^c}, \sigma_{Y^c}, \sigma_{Z^c}$ (same as $\sigma_\omega, \sigma_\phi, \sigma_\kappa$ Case 2)	.045	.086	23	10	99	30
4	$\sigma_x = \sigma_y = \pm .02$ mm. $\sigma_g = \pm 20$ m.	Same as Case 2	1.113	.146	204	16	100	30
5	$\sigma_x = \sigma_y = \pm .2$ mm $\sigma_g = \pm 2$ m	Same as Case 2	1.921	.891	348	96	100	30

point could at best be determined to within ±1.0 mm. at the 9 × 9-inch format. Research effort is being continued to study the problems of image refinement and photogrammetric calibration.

ACKNOWLEDGEMENT

The work reported in this paper has been supported by the U.S. Department of the Interior, Geological Survey. The technical support provided by Dr. Robert McEwen of the Geological Survey is gratefully acknowledged.

REFERENCES

1. Earth Resources Technology Satellite-Data Collection System, a brochure by General Electric Company, Space Division, Philadelphia, Pennsylvania.
2. Earth Resources Technology Satellite-Ground Data Handling System, Preliminary Description; a brochure by General Electric Company, Space Division, Philadelphia, Pennsylvania.
3. Earth Resources Technology Satellite-Summary System Description; NASA Goddard Space Flight Senter, Greenbelt, Maryland.
4. Forrest, Robert; Geometric Processing of ERTS Images, A paper presented at the Fall 1971 ASP-ACSM Convention, San Francisco, California.
5. McEwen, Robert; Geometric Calibration of the RBV System for ERTS, *Proceedings of the 7th International Symposium on Remote Sensing of Environment*, Vol. II, Willow Run Labs., The University of Michigan, Ann Arbor, Michigan, May 1971.
6. Wong, K. W., Geometric Distortions in Television Imageries, *Photogrammetric Engineering*, 35:5, pp. 493-500, May 1969.
7. Wong, K. W., Fidelity of Space TV, *Photogrammetric Engineering*, 36:5, pp. 491-497, May 1970.
8. Brown, D. C., Advanced Methods for the Calibration of Metric Cameras, Final Report, Part I, Contract No. DA-44-009-AMC-1457 (X), 1968, D.B.A. Systems Inc., Melbourne, Florida.